Journal of Nuclear Materials 417 (2011) 85–88

Contents lists available at ScienceDirect

Journal of Nuclear Materials

journal homepage: www.elsevier.com/locate/jnucmat

# Progress in development of CLAM steel and fabrication of small TBM in China

Qunying Huang [a,b,*], Chunjing Li [a], Qingsheng Wu [a], Shaojun Liu [a], Sheng Gao [a], Zhihui Guo [a], Zilin Yan [a], Bo Huang [a], Yong Song [a], Zhiqiang Zhu [a], Yaping Chen [a], Xinxhen Ling [b], Yican Wu [a,b], FDS Team

[a] Institute of Plasma Physics, Chinese Academy of Sciences, Hefei, Anhui 230031, China
[b] School of Nuclear Science and Technology, University of Science and Technology of China, Hefei, Anhui 230027, China

ARTICLE INFO

Article history:
Available online 22 December 2010

ABSTRACT

China Low Activation Martensitic (CLAM) steel is being developed at the Institute of Plasma Physics, Chinese Academy of Sciences under collaboration with many institutes and universities. This steel has been chosen as the primary candidate structural material for the LiPb blanket and DFLL–TBM developed in China. The development and testing strategy for DFLL–TBM includes three stages: out-of-pile tests, tests in EAST, and tests in ITER. The joining of CLAM by Hot Isostatic Pressing Diffusion Welding and Electron Beam Welding is being studied in detail, and small scale panels of the TBM first wall and cover plate with flow channels are being fabricated. Properties of CLAM including fatigue crack growth, creep properties and compatibility with liquid LiPb are also being studied. Recent progress in these R&D activities is summarized.



## 1. Introduction

Reduced activation ferritic/martensitic steels (RAFMs) steels are attractive for fusion applications because of their high level of technological maturity relative to low-activation alternatives, such as vanadium alloys and SiC composites [1–3]. Currently, RAFMs, including EUROFER97 and F82H, are considered the primary structural materials for the DEMO fusion plant and the first fusion power reactors. Research on a new version of RAFMs, China Low Activation Martensitic (CLAM) steel, started 7 years ago at Institute of Plasma Physics, Chinese Academy of Sciences (ASIPP) under collaborations with many institutes and universities [4,5]. The CLAM steel has been chosen as the primary candidate structural material for the LiPb blanket and Dual Functional Lithium Lead–Test Blanket Module (DFLL–TBM) [6–8] developed in China.

The EAST tokamak can serve as a testing platform for ITER–TBM since the basic electromagnetic parameters and the average heat flux at the first wall (FW) in EAST are comparable to those in ITER. The development and test strategy for DFLL–TBM includes three stages: tests without irradiation, tests in EAST, and tests in ITER. According to this development strategy, a series of R&D activities on CLAM and related technologies including composition design, production of the steel, impurity control, property measurement, techniques for Hot Isostatic Pressing Diffusion Welding (HIP-DW), coating, activation analysis and compilation of a database for nuclear materials, are being carried out. Initial progress was reported earlier [4].

CLAM creep properties and fatigue crack growth are being studied further. Also, joining techniques for CLAM such as HIP-DW and EBW (Electron Beam Welding) are being evaluated. Small scale panels of TBM FW and cover plate (CP) with flow channels were being fabricated. Progresses in these R&D activities are summarized in this paper.

## 2. Development of CLAM steel

Properties of CLAM steel are being widely studied and some of the new developments are summarized.

### 2.1. Fatigue crack growth

To evaluate and improve the service performance of CLAM steel under complex mechanical loads, the fatigue crack growth in CLAM steel with different quenching temperature was studied. The specimens were quenched from 930, 980 and 1030 °C, then tempered at 760 °C. Tests were carried out according to ASTM E647-1995 “Standard test method for fatigue crack growth rates of metallic materials”.

The dependence of fatigue crack growth rate on quenching temperature is shown in Fig. 1. The fatigue crack growth curve describes the Paris region of stable growth of CLAM steel. It shows that the fatigue crack growth rate of CLAM steel for quenching temperature of 980 °C and 1030 °C are similar. The crack propagation rate increased quickly when the quenching temperature was 930 °C. This can be explained as follows: the high quenching tem-

* Corresponding author at. Institute of Plasma Physics, Chinese Academy of Sciences, Hefei, Anhui 230031, China. Tel./fax: +86 551 5593328.
E-mail address: qyhuang@ipp.ac.cn (Q. Huang).

0022-3115/$ - see front matter Crown Copyright © 2010 Published by Elsevier B.V. All rights reserved.
doi:10.1016/j.jnucmat.2010.12.170

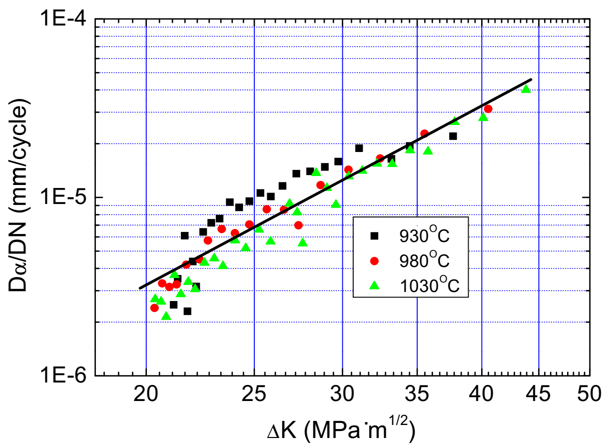


**Fig. 1.** Fatigue crack growth rate, $d\alpha/dN$, vs. amplitude of stress, $\Delta K$.

perature reduced the segregation of impurities at prior austenite grain boundaries which improved the intragranular strength. In addition, grain coarsening during normalizing was also one of the possible reasons for the slow propagation rate.

### 2.2. Creep tests of CLAM steel

Uniaxial creep tests of CLAM (HEAT 0603A) and JLF-1 (JOYO-2-HEAT) steels were systematically investigated at test temperatures from 550 °C to 650 °C with applied stresses of 100–300 MPa using the Japanese small tensile specimens (SSJ) small specimens [9–11]. In all cases, the creep curve displayed normal behavior, similar to other RAFMs, where at constant temperature (or stress), the deformation rate increased and the secondary stage was reduced with an increase of the applied stress (or temperature). By extrapolating to typical blanket condition (e.g. 550 °C for 100,000 h) using the Larson–Miller parameter, the rupture stress was estimated to be about 140 MPa for both steels [10], which is comparable to other RAFMs [12].

The effects of thermal ageing on mechanical properties and microstructure were also studied [9]. Ageing at 550 °C for 2000 h caused a slight increase in hardness and improvement of creep properties. However, properties were degraded after ageing at 700 °C for 100 h. Comparing these two steels, CLAM has higher hardness, tensile and creep strength, but is more susceptible to thermal ageing than JLF-1. The lower heat treatment temperature, leading to finer grain size and smaller lath width, was believed to be the main reason for higher hardness, higher strength, and susceptibility to ageing of CLAM than for JLF-1. [11].

### 2.3. Compatibility with liquid LiPb

Previous studies of corrosion of CLAM steel in flowing LiPb showed that CLAM has good compatibility under thermal convection flow at 480 °C for more than 5000 h [13–15]. Analysis of the specimens exposed to liquid LiPb for 10,000 h is underway. Based on the previous results, specimens with and without coating and specimens for tensile tests were exposed to LiPb in a DRAGON-ST capsule at 550 °C for more than 5000 h. After dissolution of protective oxides $(Fe,Cr)_2O_3$ was confirmed by X-ray diffraction, severe corrosion attack was observed at the interface between the liquid metal and the matrix [16]. The CLAM steel exhibited a linear trend of weight loss with increasing exposure time at 550 °C, consistent with results obtained on other RAFMs [17].

The tensile properties of CLAM steels exposed to flowing LiPb at 480 °C for 3000 h and exposed to static LiPb at 550 °C for 5000 h were evaluated. The results obtained at 480 °C showed that the ultimate tensile strength (UTS) and the total elongation (TE) both decrease slightly compared with results for unexposed specimens. For the specimens exposed at 550 °C, the trend of UTS and TE indicated that the tensile properties were almost unaffected by the exposure to LiPb for 5000 h. However, it is still necessary to do experiments for liquid LiPb corrosion while in a neutron irradiation environment.

### 2.4. Irradiation resistance of CLAM

Neutron and ion irradiation tests to investigate properties of CLAM after irradiation, have been carried out in collaboration with many Chinese and overseas institutions. Tensile and impact tests after neutron irradiation to 0.02 dpa at 250 °C showed slight increases of strength and DBTT shift [18]. Fluorine ion irradiations to 80 dpa at room temperature have been conducted and irradiation induced defects are being investigated by slow positron beam and microstructure observations. These data will be used to better understand the irradiation hardening. In addition, microstructural evolution during electron irradiation at 450 °C and 500 °C was investigated using high voltage electron microscope (HVEM) [19].

## 3. Joining techniques and fabrication of blanket mock-up

Major steps in the fabrication of DFLL-TBM include manufacturing of the FW, the cooling plates (CP) and the assembly of these components. EBW, tungsten inert gas (TIG) welding, and laser welding are candidate welding techniques for the joining of FW and CPs.

### 3.1. Fusion welding techniques

Fusion welding techniques are being developed for TBM fabrication. Also, thermal simulations using a Gleeble machine were performed to assist the optimization of fusion welding techniques.

CLAM plates 11 mm thick were EB welded by KLL-100 with welding parameters of 60 kV, 70 mA, 600 mm/min, without preheating or post-weld heat treatment. Good penetration joints were obtained. Microstructures of a joint of CLAM steel produced by EB are shown in Fig. 2. Fig. 2a shows that it was difficult to observe defects (such as pores) in macrograph of the cross-section of the joint. The microstructure of the fusion zone was lath Martensite, shown in Fig. 2b.

Mechanical properties of the joints were measured following established standards (national standard of the People's Republic of China, such as GB/T2651-2008 and GB/T2654-2008). The UTS of the joint was 655 MPa, and all fractures were located in the base metal. At the same time, the maximum hardness was HV453, located in the center of the fusion zone. This hardness was too high,

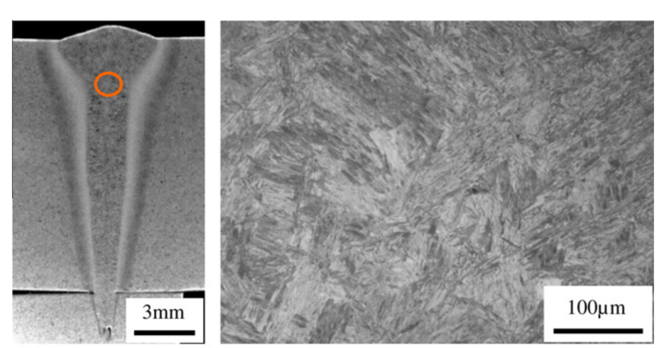


(a) Macrograph (b) Micrograph of the weld

**Fig. 2.** Microstructures of a CLAM steel joint produced by Electron Beam Welding.

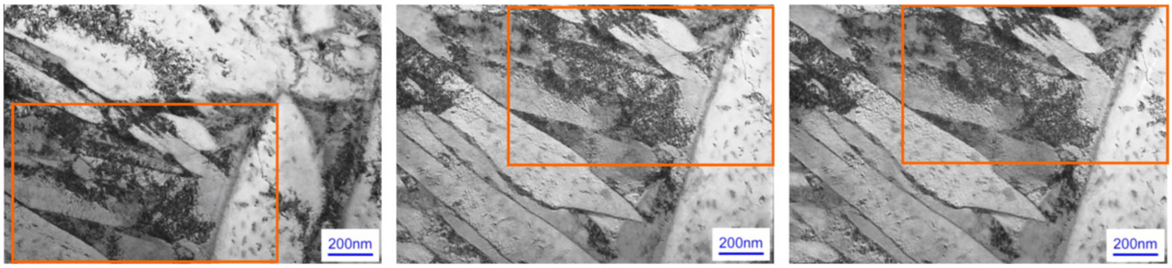


**Fig. 3.** Micrograph of CLAM welding specimen irradiated at 450 °C with electron beam.

compared to HV220 of the bulk material. Further experiments to reduce the hardness of the weld center will be performed including post-weld heat treatment of the joints.

Using the HVEM (JEM-ARM1300) in the Graduate School of Engineering, Hokkaido University, an electron beam irradiation experiment in the fusion zone of the joint was performed at 450 °C to irradiation doses of 0–8.4 dpa. During the irradiation, the microstructure was observed in situ with examples shown in Fig. 3. It was difficult to observe changes in the microstructure of the weld, even at irradiation doses up to 8.4 dpa.

Manual gas tungsten arc welding experiments of 4 mm plate were performed using CLAM filler wire of 2 mm diameter taken from the same plate. The weld groove was V-type with 60° angle. One weld used preheating to 150 °C and one weld had no preheating. The double-bead lap joints were tempered at 760 °C for 30 min after the welding to improve the mechanical properties. X-ray inspection showed that they are grade I joints without significant defects. Metallographic observation showed the joints are lath Martensite. The fusion zone grain size was obviously coarsened, especially in the weld made without preheating.

Some preliminary laser welding experiments of CLAM have been done and the results are being analyzed.

Thermal simulation experiments of CLAM fusion welding using a Gleeble were carried out to assist the development of fusion welding techniques. The Hannerz method was used to control heating and cooling of CLAM sample. Parameters include a maximum temperature of 1350 °C, preheating to 100 °C and cooling time from 800 °C to 500 °C. The results show that the microstructure of all samples is lath Martensite and the grain size increases with the time cooling from 800 °C to 500 °C.

### *3.2. Fabrication technique for key components with flow channels*

HIP-DW is a promising technology to fabricate components with complex cooling channels for ITER–TBM due to the advantages associated with avoiding melting. HIP-DW experiments on CLAM have been performed and good joints were obtained through the optimization of HIP conditions [20]. The primary fabrication technique for the FW is HIP-DW of two plates with a rectangular tube. The CLAM steel rectangular tubes and small plane mockup are being fabricated to study the fabrication techniques of the FW. A one-fifth scale FW mockup will be manufactured based on these techniques. Details for fabrication techniques for key components with flow channels are presented elsewhere and can be referred to Refs. [20–22].

## 4. Coatings on CLAM

Coating of the structural CLAM steel is proposed as the primary solution to some key issues, including tritium permeation and leakage, magnetohydrodynamic (MHD) effects, and compatibility with liquid LiPb in a liquid LiPb blanket [23].

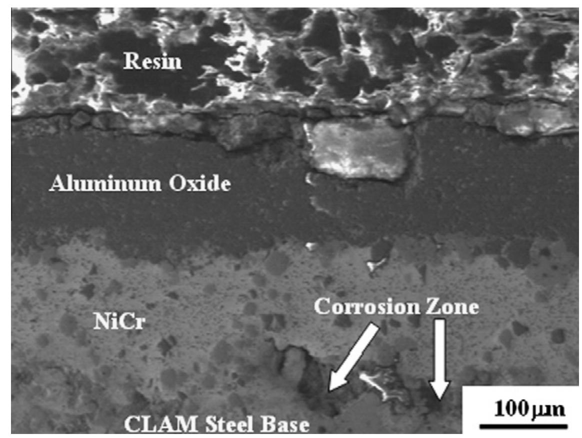


**Fig. 4.** NiCr/$Al_2O_3$ coatings after 5000 h exposure in 550 °C LiPb.

$Al_2O_3$ is the candidate coating material in FDS series designs. Because of the complicated geometry of the LiPb blanket, development of coatings has focused on $Al_2O_3$ formed on CLAM steel aluminized by Hot-Dip Aluminizing (HDA) and Chemical Vapor Deposition (CVD). Coatings produced by CVD at 700 °C have uniform thickness, dense structure, high aluminum composition, high micro-hardness, high electrical resistivity and a pure $Al_2O_3$ surface layer [24]. A 0.8 μm thick $Al_2O_3$ coating containing $\gamma$-$Al_2O_3$ on aluminized CLAM steel was produced by HDA followed by oxidation at 900 °C in $O_2$ [25]. A vacuum plasma sprayed (VPS) functionally graded $Al_2O_3$ coating showed good adhesion compared with a non-graded $Al_2O_3$ coating. Thermal shock resistance tests showed that the graded coatings were sound after 30 cycles of thermal shock at 600, 700, and 800 °C, while the non-graded coating peeled off after 29 and 15 cycles of thermal shock at 700 and 800 °C respectively. In addition, NiCr/$Al_2O_3$ coatings were prepared with atmospheric plasma spray (APS) on CLAM (HEAT 0603B), with NiCr as the bonding layer. The coating was exposed to liquid LiPb at 550 °C for 5000 h to study the compatibility [26]. The results (shown in Fig. 4) indicated that there is no obvious thinning of the external layer aluminum oxide, and the damage to the coating seemed to start at the edge of the internal layer of NiCr by dissolving Ni in liquid LiPb.

$Al_2O_3$ is considered the primary candidate coating material for LiPb blankets, while research on other coating materials, such as SiC, is underway. In addition, research on a multilayer coating such as $Al_2O_3$ + SiC on CLAM for use in LiPb blankets is also ongoing.

## 5. Summary

A series of R&D on the structural material CLAM and related technologies are being carried out at ASIPP in extensive collaboration with other institutes and universities in China and overseas.

Through these efforts the main achievements of research on CLAM steel have occurred in the following areas:

(1) the mechanical properties of CLAM including crack propagation rate, creep rate and compatibility with LiPb are better known;
(2) welding techniques HIP-DW and EBW of CLAM were studied and good joints have been obtained. Fabrication of a one-fifth scale TBM mockup has started;
(3) research on coating techniques on CLAM steel has started.

Development of CLAM is being supported by an increasing number of projects. Much more R&D on CLAM and TBM fabrication technologies will continue to be carried out to meet the Quality Assurance requirement of TBM. As a result of this need, the speed of CLAM development will be greatly accelerated.

## Acknowledgements

This work was supported by the China National Natural Science Foundation with Grant Nos. 10775135, 50805138, 50871108, and 10975157, the National Basic Research Program of China with Grant Nos. 2009GB109000 and 2009GB104005, and the Knowledge Innovation Program of Chinese Academy of Sciences.

## References

[1] S. Jitsukawa, A. Kimura, A. Kohyama, et al., J. Nucl. Mater. 329–333 (2004) 39–46.
[2] N. Baluc, D.S. Gelles, S. Jitsukawa, et al., J. Nucl. Mater. 367–370 (2007) 33–41.
[3] R.J. Kurtz, A. Alamo, E. Lucon, et al., J. Nucl. Mater. 386–388 (2009) 411–417.
[4] Q. Huang, C. Li, Y. Li, et al., J. Nucl. Mater. 367–370 (2007) 142–146.
[5] Q.Y. Huang, Y.C. Wu, J.G. Li, et al., J. Nucl. Mater. 386–388 (2009) 400–404.
[6] Y. Wu, The FDS Team, Nucl. Fusion 47 (2007) 1533–1539.
[7] Y. Wu, The FDS Team, Fusion Eng. Des. 82 (2007) 1893–1903.
[8] Y. Wu, The FDS Team, J. Nucl. Mater. 367–370 (2007) 1410–1415.
[9] Y.F. Li, T. Nagasaka, T. Muroga, et al., J. Nucl. Mater. 386–388 (2009) 495–498.
[10] Yanfen Li, T. Nagasaka, T. Muroga, Long-term thermal stability of reduced activation ferritic/martensitic steels as structural materials of fusion blanket, in: Presented at the 18th International Toki Conference (ITC-18), Toki, Gifu, Japan, December 9–12, 2008.
[11] Yanfen. Li, T. Nagasaka, T. Muroga, Fusion Sci and Tech 56 (2009) 323–327.
[12] R. Lindau, A. Moslang, M. Schirra, Fusion Eng. Des. 61–62 (2002) 659–664.
[13] Qunying. Huang, Sheng. Gao, Zhiqiang. Zhu, et al., Fusion Eng. Des. 84 (2009) 242–246.
[14] Q. Huang, M. Zhang, Z. Zhu, et al., Fusion Eng. Des. 82 (2007) 2655–2659.
[15] M. Zhang, Q. Huang, Y. Wu, et al., Mater. Sci. Forum 561–565 (2007) 1741–1744.
[16] S. Gao, Q. Huang, Z. Zhu, et al., Corrosion and mechanical behavior of CLAM steel in liquid LiPb at 480 °C and 550 °C, in: Presented at the 14th International Conference on Fusion Reactor Materials (ICFRM-14), Sapporo, Japan, September 7–12, 2009.
[17] H. Glasbrenner, J. Konys, H.D. Rohrig, et al., J. Nucl. Mater. 283–287 (2000) 1332–1335.
[18] L. Peng, Q. Huang, C. Li, S. Liu, J. Nucl. Mater. 386–388 (2009) 312–314.
[19] L. Peng, Q. Huang, Y. Wu, et al., Chin. J. Atomic Energy Sci. Technol. 41 (Suppl.) (2007) 106–111.
[20] C. Li, Q. Huang, Q. Wu, et al., Fusion Eng. Des. 84 (2009) 1184–1187.
[21] B. Hunag, C. Li, S. Liu, S. Liu, Chin. J. Nucl. Sci. Eng. 30 (2007) 59–64.
[22] Q. Huang, Q. Wu, C. Li, et al., Fusion Eng. Des. 85 (2010) 2192–2195.
[23] Y. Wu, The FDS Team, J. Nucl. Mater. 367–370 (2007) 1410.
[24] X. Li, G. Yu, J. Yu, et al., J. Nucl. Mater. 329–333 (2004) 1407.
[25] S. Han, H. Li, S. Wang, et al., Int. J. Hydrogen Energy 35 (2010) 2689–2693.
[26] Z. Guo, Q. Huang, Z. Yan, et al., Fusion Eng. Des. 85 (2010) 1469–1473.